LOAD TRANSFER MECHANISM OF GEOCELLS

A. Emersleben
Department of Geotechnical Engineering, Clausthal University of Technology, Germany
Tel: +49-5323 72 3699; Fax: +49-5323 72 2479; E-Mail: Ansgar.Emersleben@tu-clausthal.de

ABSTRACT

The lack of common usable design models for the design of geocell stabilized soils is mainly based on the small knowledge about the load transfer mechanism within a geocell system. To evaluate the load transfer mechanism within a geocell system, a new test device was constructed to evaluate the interaction between hoop stresses in the cell walls and passive earth resistance of single and multiple geocells. Based on the results of the radial load tests an analytical model was developed to describe the load transfer mechanism within a geocell system. The model was used to develop a common usable design model for serviceability and limited state analysis of geocell stabilized soils. Radial load tests, analytical model for load transfer mechanism with a geocell system and design model for serviceability analysis are described in the paper.

Keywords: Geocells, cellular confinement, soil stabilization, reinforcement

INTRODUCTION

The construction of bound and unbound infrastructure projects over weak subsoil requires high technical requirements on the construction and the design of the different layers involved. Under bound layers usually thick layers are constructed to satisfy settlement requirements. The thick layers distribute the stresses from the traffic and lead to a uniform pressure on the subsoil ensuring the specified settlement criteria. However, construction of thick base layers is due to height restrictions or economical reasons not always possible. In these cases engineering improvements of the subsoil properties represents a possibility to ensure the specified requirements. The possible construction methods to improve the subsoil are manifold and depend on the chosen construction. Soil replacement, cement or lime stabilization or support by pile-like elements can be used. Especially in unbound roads the use of geosynthetics is increasingly used as an alternative to traditional construction methods. Geotextiles are mainly used to separate subsoil and base layer and therefore result in an improved compaction of the base layer. Single geogrid layers result in an improved compaction and additionally absorb horizontal stresses due to the activation of tensile stresses within the geogrid.

Geocells represent an alternative for the stabilization of low bearing capacity soils under bound and unbound infrastructure projects. Geocells are three-dimensional connected cells which form a honeycomb structure. The geocells are stretched on the place of installation, filled with infill material and compacted. If the geocells are vertical loaded strains in the cell walls and earth resistance in the adjacent cells are mobilized leading to reduction of horizontal deformations of the infill material. Due to the horizontal embedment by the geocell walls the stiffness of the stabilized soil is increased and the applied loads are distributed over a wider area leading to reduction of settlements e.g. Emersleben and Meyer 2008, Sitharam et al. 2008).

Comparable to the design of geogrid reinforced soils no common usable design concept is available for the design of geocell stabilized soils at the moment. This is mainly based on lack of detail information about the load transfer mechanism within the geocell system. Many different static and dynamic load tests have been carried out to evaluate the influence of geocells on the load-deformation behavior of different soils (e.g. Sitharam 2008, Mhaiskar and Mandal 1993). In addition in-situ tests sections were carried out to evaluate the influence of geocell stabilization on the long-term performance of unpaved and paved roads e.g. (Emersleben 2010, Hughes 1999). Triaxial tests on single geocells were carried out by e.g. Bathurst et al. (1988), Wesseloo (2009) to evaluate the influence of geocells on the shear properties of the infill material. Due to those tests the influence of geocells on load-deformation behavior and the overall performance of different soils and pavement constructions are well known, but neither load tests, in-situ tests nor triaxial tests on single geocells are adequate to evaluate the load transfer mechanism within a geocell system, which consists of many interconnected single geocells. Especially the interaction of connected individual cells within the geocell structure and the resulting horizontal resistance dependent of the activated strains within the geocell walls cannot be investigated by static or dynamic vertical box load

tests or triaxial tests on single cell. Because of that the design of the geocell stabilized soil is mainly based on experience or very simplistic design methods to estimate the ultimate bearing capacity. Design models for serviceability analysis do not exist at the moment.

Within this publication laboratory tests are described that investigated the interaction of activated geocell strains and horizontal resistance as a function of number of surrounding cells as well as different geocell parameters such as height, material stiffness and thickness of the overlying material. For this purpose a new test called radial load tests (RLT) were conducted.

RADIAL LOAD TESTS

Test Setup

The radial load tests described are loaded by a pneumatic pressure bag which applies horizontal pressures on a single cell. The air pressure bag consists of an air filled membrane with an internal steel cylinder. The steel cylinder prevents that the pressure cell applies internal stresses and ensured a uniform stress application on the geocell walls. The pressure bag has a height and diameter of 250 mm and 200 mm respectively. The dimensions of the pressure bag were optimised to investigate 150 mm high cells with a diameter between 200 and 230 mm. However, radial tests were also conducted with 100 and 200 mm high cells. The pressure bag is controlled by an electronic valve which is controlled by an automatic control program. Static tests can be executed in a load- or strain-controlled way up to 500 kPa. For the test setup the air pressure bag was installed in the centre of the test box. The box had a height of 300 mm and a width and length of 1270 mm to avoid interactions of the measurement devices and test materials with the side walls. A vertically movable base plate was constructed to ensure that geocells with different heights can be loaded centrally by the air pressure bag (Fig. 1). This also allowed installation of soil embedment in different heights. A rough surface of the base plate ensured that the friction angle of the fill material and the friction angle of base plate and soil are comparable. Preliminary tests indicated that the test conditions allow a good correlation of determined interface friction angle and the soil friction angle.

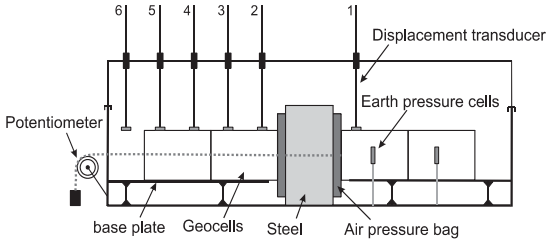

Fig. 1 Schematic cross section of radial load tests.

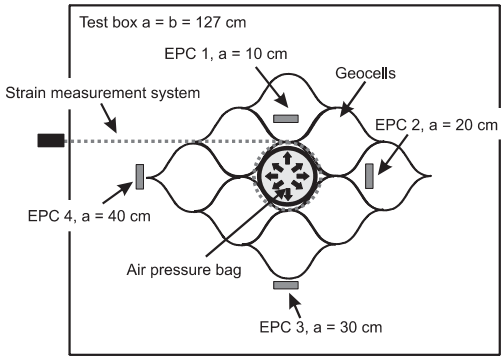

Fig. 2 Schematic plan of radial load tests.

Indirect strains measurements were incorporated by using a rotary potentiometer. Strains were measured by a string with plastic properties placed around the loaded cell. From the elongation the activate geocell strains were analyzed.

In addition to cell strains the horizontal earth pressure in the fill material was measured at different distances to the loaded cell. Four earth pressure cells (EPC) were placed with a distance of a = 100 mm, 200 mm, 300 mm and 400 mm from the loaded cell. Based on the symmetrical test arrangement the earth pressure cells were installed at different positions around the loaded cell to prevent interaction of measurement devices (Fig. 2).

The earth pressure cells are based on strain gauges measurements and allow identification of cyclic loads. Due to the size (50 mm diameter) they have only small influence on the soil pressure distribution. The earth pressure cells were vertically positioned in mid-height of the geocell. The clamps were connected to the test box by steel springs which avoid stress concentration after large soil displacements occurred. Surface deformations were measured in selected tests by inductive displacement transducers. Two displacement transducers (No. 1 and 2) were symmetrically positioned at 100 mm distance to the edge of the tested cell. All other displacement transducers were placed with an internal distance of 110 mm (Fig. 1) and connected to a measuring bridge. Measurement data was automatically collected by a measurement amplifier in combination with a software package.

Soil and Geocell Materials

Uniformly graded river sand with effective particle size (D10) of 0.23 mm, maximum dry unit weight of 18.8 kN/m³ and minimum dry unit weight of 14.5 kN/m³ was used in the experiments. All tests were carried out at 81 % relative density of sand. The average peak angle of friction of sand at installation density as determined from direct shear tests is 41°. Additional conducted compression tests for the sand indicated for the installation density of 1.8 g/cm³ and pressures up to 200 kN/m² stiffness modulus between 20 and 50 MN/m². To ensure constant and reproducible boundary conditions in the tests the described fill materials were installed at dry conditions. The relevant soil mechanical properties of the sand are given in Table 1.

Table 1 Mechanical properties of used soil.

Description	Sand SE
Grain density (g/cm³)	2.65
Installation density (g/cm³)	1.80
Relative density D	0.81
Minimum dry unit weight (g/cm³) (DIN 18 126)	1.45
Maximum dry unit weight (g/cm³) (DIN 18 126)	1.88
Proctor density (at optimum water content) (g/cm³)	1.77
Optimum water content (%)	9.3
Friction angle at installed density	41°

Geocells from three different manufacturers were used in the experiments. The geocells can be differentiated by their manufacturing process as well as the used raw material. Geocells made out of a high density polyethylene (PEHD), a thermally bonded nonwoven and a mixture of PEHD and polyester (PES/PEHD) with different tensile strengths were used. The use of geocells made out of different raw materials was mainly considered for the variation of tensile stiffness. Besides the stiffness the used materials have a different surface texture. The rough structure of the surface of the PEHD geocells was achieved by 22 to 31 0.35 – 0.85 mm deep sinking's per cm². Additionally perforated PEHD cells were used were in addition to the structured surface holes with a diameter of 10 mm were punched into the cell material. The opening area of the holes represents 16 % of the cell area. The surface structure of the PES/PEHD cells is smooth while the geocells made of a non-woven is rough.

For the determination of the geocells stress-strain properties tensile tests in accordance to DIN EN ISO 10319 were conducted. The tested PEHD geocellswith a smooth and a perforated surface showed a significant difference in the stress-strain properties despite a comparable manufacturing process and identical raw material. It was concluded that this is a result of the perforation within the geocell structure and the resulting stress distribution within the cell area. An overview of the used geocells and the relevant material parameters is given in Table 2.

Table 2 Material properties for the used geocells.

	PEHD perforated	PEHD smooth	Thermally bonded nonwoven	PES /PEHD
Notations	PEHD perf. orig.	PEHD glatt orig.	PES-V orig.	PES/PEHD glatt orig.
Material surface	structured, perforated	structured	smooth	smooth
Ultimate tensile force [N/cm]	175	206	206	259
Strain at failure [%]	15	10	28	12

ANALYTICAL MODEL OF LOAD TRANSFER MECHANISM

The radial load tests have shown that the load transfer mechanism of geocells essentially consists of hoop stresses in the cell walls, mobilized lateral earth pressure due to the surrounding soil and mobilized lateral earth pressure due to the adjacent geocells. The interaction between hoop stresses in the cell walls and passive lateral earth pressure is not considered in the current calculation methods and design of geocell stabilized structures. Besides, insufficient research work of the interaction of single load transfer mechanisms (hoop stresses and passive earth pressure) did not allow a quantification of single parameters on the load transfer mechanism up to now. With the help of the radial load tests the influence of different parameters on the load transfer behavior has been evaluated and the relation between single load transfer mechanisms has been described and quantified. On basis of these results an analytical model of the interaction of the single load transfer mechanisms can be developed. This model is described in the following.

Analytical modelling is based on the consideration of a horizontally loaded geocell. This consideration is in accordance with the radial load tests. The influence of a vertical load on the geocell is neglected firstly and considered in the model later on. If a radial-symmetrical horizontal load (σ_h) is applied within a single cell of a geocell system, lateral resistance ($\sigma_{h,geo}$) is mobilised as a result of the hoop tensile stresses within the geocell wall (σ_r). The amount of mobilized hoop stresses depends on

the stiffness and the stress-strain behaviour of the geocell material. In addition to the lateral bedding due to hoop stresses the surrounding soil generates a lateral bedding effect ($\sigma_{h,B}$) until a horizontal equilibrium has been developed in the overall system. In addition, the radial load tests have shown that further bedding component ($\sigma_{h,G}$) is mobilised by the adjacent geocells (Fig. 3).

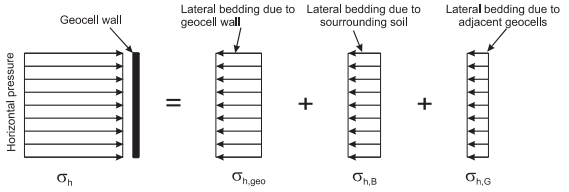

Fig. 3 Horizontal stress equilibrium in the geocell system at horizontal loading of a single cell within the geocell system.

The modeling was accomplished based on a structure of an unconfined single cell to a complex geocell system filled with sand. The analytic model was verified for each case by a comparison with the results of the radial load tests on 15 cm high geocells. In the following only the final analytical model for the whole geocell system is presented. By using the hoop tensile force for the geocell material, which was determined by testing single unconfined geocells in the RLT-tests the stress equilibrium (Fig. 3) can be expressed according to Eqs. 1 and 2.

$$\sigma_{h(\varepsilon<1\%)} = \frac{F_{rad(\varepsilon)} \cdot 2 \cdot t}{d_{(\varepsilon,r)} \cdot A} + \frac{1}{2} \cdot \gamma \cdot z \cdot \frac{\varepsilon}{0,01} \cdot k_{pgh} \cdot \mu_E + c \cdot \frac{\varepsilon}{0,01} \cdot k_{pch} \cdot \mu_C \quad (1)$$

$$\sigma_{h(\varepsilon\geq1\%)} = \frac{F_{rad(\varepsilon)} \cdot 2 \cdot t}{d_{(\varepsilon,r)} \cdot A} + \frac{1}{2} \cdot \gamma \cdot z \cdot k_{pgh} \cdot \mu_E + c \cdot k_{pch} \cdot \mu_C \quad (2)$$

with $$d_{(\varepsilon,r)} = d_0 + \varepsilon_r \cdot d_0 \quad (3)$$

with $$F_{(rad,\varepsilon)} = E \cdot A \quad (4)$$

with $F_{rad(\varepsilon)}$ calculated hoop tensile force from the RLT test; $d_{(\varepsilon,r)}$ adapted geocell diameter according to equation 3; μ_E factor for the consideration of the spatial earth pressure; μ_C factor for the consideration of the spatial earth pressure due to spatial cohesion; c adherent cohesion; ε_r measured strain/elongation in radial load test; E secant modulus at 5 % strain on basis of radial load tests on single unconfined geocells; A cross section area of geocell.

A calculation of the acceptable horizontal pressure after Eqs 1 or 2 illustrates the influence of the junctions on the stress-strain behavior and therefore on the horizontal pressure of a single geocell within a geocell system. A calculation of the acceptable horizontal pressure for geocell heights of 100 mm and 200 mm shows a very good correspondence with the test results (Figs. 4 and 5).

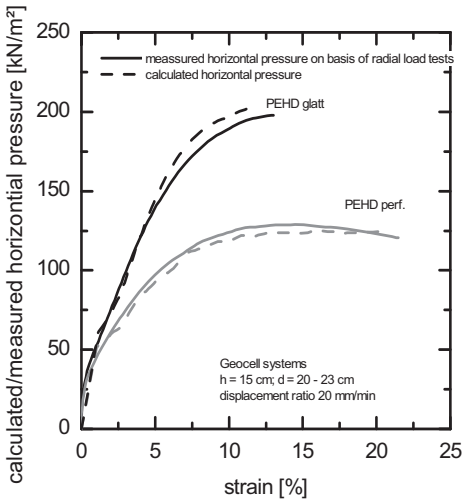

Fig. 4 Comparison between calculated horizontal pressure after Eqs. 1 and 2 and measured horizontal pressure in radial load tests for smooth and perforated PEHD geocells.

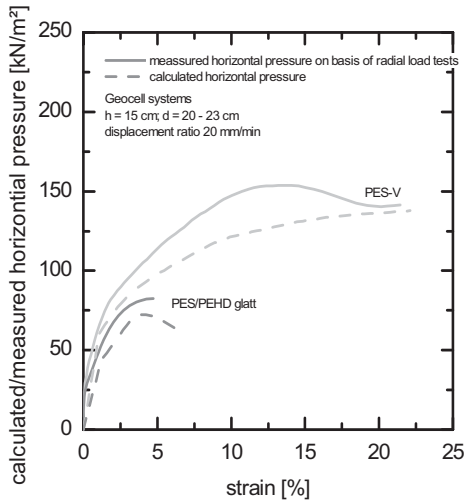

Fig. 5 Comparison between calculated horizontal pressure after Eqs 1 and 2 and measured horizontal pressure in radial load tests for PES and PES/PEHD geocells.

DESIGN MODELL

Vertical Load Tests

To transfer the results gained from the radial load tests on the real loading situation within a geocell stabilised system under an unbound traffic are additional investigations of the influence of vertical loads on the interaction behaviour within the geocells is required. A comparison of results from radial- and vertical load tests allow subsequently a control on the transferability of the conclusions drawn from the radial load tests on the vertical loading and allow on the other hand the development of a model to describe the connection between horizontal and vertical load within a loaded geocell.

The test setup and the execution of the vertical strain tests differ from the radial load tests due to the direction of the applied load. While in the radial load tests a horizontal load is applied by an air-pressure bag within a single cell, the vertical strain tests are executed by a vertical load of a hydraulic piston with a maximum capacity of 100 kN. A stiff plate (d = 210 mm) ensures load transfer from hydraulic piston on the geocells. The loading plate deformations were measured by inductive displacement transducers with a nominal range of 300 mm. Comparable to the radial load tests a test box with a height of 30 cm, length and width of 1.27 m was used. The type and arrangement of the used measurement devices to measure horizontal stresses within the soil (earth pressure cells) and strains within the loaded cell (potentiometer) were chosen as in the radial load tests. The use of similar boundary conditions ensures that the results can be compared easily. A schematic overview of the test set-up is given in Fig. 6.

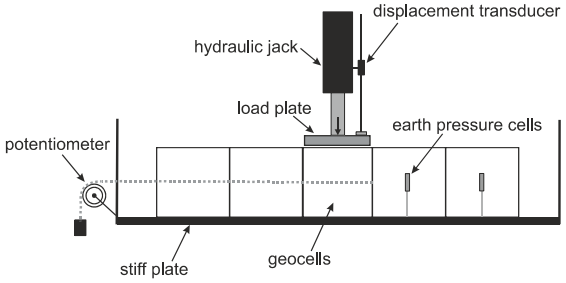

Fig. 6 Schematic cross section of the test setup for the vertical load test.

Calculation of Maximum Vertical Stresses with a Geocell System

The verification of the analytical model using the radial load test results demonstrated that the model can be used to calculate sand filled horizontally loaded geocell systems. The relationship between existing horizontal stresses and vertical loads within a geocell structure was derived based on laboratory radial and vertical strain tests while the subsoil influence was neglected. The comparison indicates that horizontal stresses in a vertically loaded geocell structure can be calculated by traditional soil mechanics (Eq. 5).

$$\sigma_{v(\varepsilon)} = \frac{\sigma_{h(\varepsilon)}}{k_{agh}} \tag{5}$$

Using the strain dependent hoop tension force within a single geocell $F_{(rad,\varepsilon)} = E * a * \varepsilon$, the maximum horizontal stress in a single loaded cell can be calculated dependent on the strain level based on equation 6 and 7.

$$\sigma_{h(\varepsilon<2\%)} = \frac{2 \cdot E \cdot a \cdot \varepsilon \cdot t}{(d_0 + \varepsilon \cdot d_0) \cdot A} + \frac{1}{2} \cdot \gamma \cdot z \cdot \frac{\varepsilon_{(<2\%)}}{0,02} \cdot k_{pgh} \cdot \mu_E + c \cdot \frac{\varepsilon_{(<2\%)}}{0,02} \cdot k_{pch} \cdot \mu_C \tag{6}$$

$$\sigma_{h(\varepsilon\geq 2\%)} = \frac{2 \cdot E \cdot a \cdot \varepsilon \cdot t}{(d_0 + \varepsilon \cdot d_0) \cdot A} + \frac{1}{2} \cdot \gamma \cdot z \cdot k_{pgh} \cdot \mu_E + c \cdot k_{pch} \cdot \mu_C \tag{7}$$

with d_0 geocell diameter at installation; μ_E factor for the consideration of the spatial earth pressure; μ_C factor for the consideration of the spatial earth pressure due to spatial cohesion; c adherent cohesion; ε_r geocell strain; E secant modulus at 5 % strain on basis of radial load tests on single unconfined geocells; A cross section area of geocell with perforations; z cell height plus soil cover thickness above the geocells; γ unit weight of the infill material; a cross section area of geocell considering the perforation; t thickness of the geocell material.

Figures 7 and 8 compare the calculated maximum horizontal stresses according to equations 6 and 7 and laboratory vertical stress test results using three different geocell material types. For stresses up to 600 kN/m² a good correlation can be established between numerical and physical tests. For stresses in excess of 600 kN/m² variations are noted which is a result of the interaction of the stiff loading plate and the rigid subsoil. The calculated stresses however underestimate the maximum load and can therefore be used for the design. Differences in the calculation and physical tests of the PES-V geocells however are due to material variations. Especially the radial load tests showed reduced stress-strain behaviour due to debonding of different layers of the geocell material.

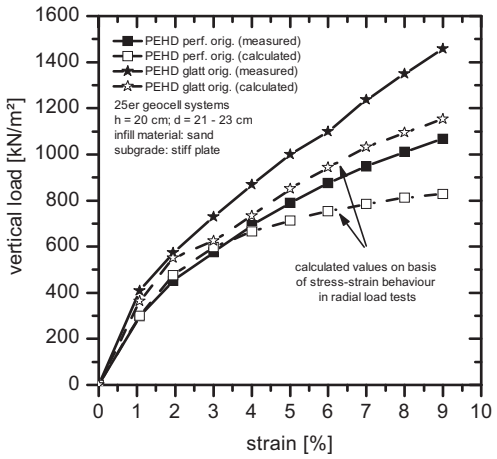

Fig. 7 Comparison of calculated vertical stresses according to equation 6 and 7 and measured vertical stresses for perforated and smooth PEHD geocells.

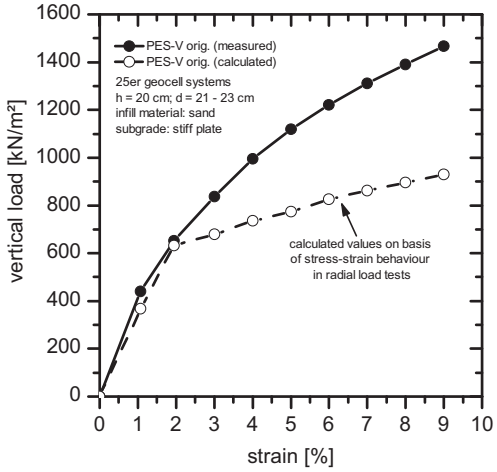

Fig. 8 Comparison of calculated vertical stresses according to equation 6 and 7 and measured vertical stresses for PES-V geocells.

Neglecting the subsoil influence, the presented results indicate that maximum vertical stresses of a geocell system can be calculated according to equations 6 and 7 for any given strain. Transposing equations 6 and 7 allow different parameters than the vertical stress to be calculated.

Calculation of Settlement within the Geocells

Assuming no volumetric change within a loaded single cell, the settlement within the geocell and the geocell strains are linked up according to equations 8, 9 and 10.

$$s_{G,b} = \left(1 - \frac{{d_0}^2}{\left(d_0 + \varepsilon \cdot d_0\right)^2}\right) \cdot h_0 \qquad (8)$$

With $s_{G,b}$ settlements within the geocell layer; d_0 geocell installation diameter; ε geocell material strain dependent on vertical stress; $h_0$geocell height at installation

The load dependent strain ε is calculated based on Eq. 9 for a strain level up to 2%.

$$\varepsilon_{(<2\%)} = -\frac{\left(\frac{2 \cdot t \cdot a \cdot E + a_1 + a_2 - a_3}{\left(a_1 + a_2\right)}\right)}{2} + \sqrt{\left(\frac{\left(\frac{2 \cdot t \cdot a \cdot E + a_1 + a_2 - a_3}{\left(a_1 + a_2\right)}\right)}{2}\right)^2 + \frac{a_3}{\left(a_1 + a_2\right)}} \qquad (9)$$

with $$a_1 = \frac{1}{0,04} \cdot \gamma \cdot z \cdot k_{pgh} \cdot \mu_E \cdot d_0 \cdot A \qquad (10)$$

$$a_2 = \frac{1}{0,02} \cdot c \cdot k_{pch} \cdot \mu_c \cdot d_0 \cdot A \qquad (11)$$

$$a_3 = \left(\sigma_v \cdot k_{pgh}\right) \cdot d_0 \cdot A \qquad (12)$$

For strains in excess of 2 % the load dependent strain is calculated based on Eq. 13:

$$\varepsilon_{(\varepsilon \geq 2\%)} = \frac{\left(\sigma_v \cdot k_{agh} - b_1 - b_2\right) \cdot d_0 \cdot A}{\left[E \cdot a \cdot 2 \cdot t - \left(\sigma_v \cdot k_{agh} - b_1 - b_2\right) \cdot d_0 \cdot A\right]} \qquad (13)$$

with $$b_1 = \frac{1}{2} \cdot \gamma \cdot z \cdot k_{pgh} \cdot \mu_E \qquad (14)$$

$$b_2 = c \cdot k_{pch} \cdot \mu_c \qquad (15)$$

Figures 9 and 10 compares the calculated (Eqs 9 and 13) geocell settlements with the results of laboratory vertical stress tests for perforated and non-perforated PEHD geocells. A good correlation between calculated and measured values is noted. For stresses up to 700 kN/m² a difference of only 5 mm is noted between measured and calculated geocell settlements. For vertical stresses in excess of 800 kN/m² calculated settlements of perforated PEHD geocells are larger than measured settlements as interaction effects of loading plate and stiff base plate influence the measured stresses. This interaction prevents settlements within the geocell layer. The material behavior observed in the radial stress tests is however fully incorporated in the calculation. The settlement calculation therefore results in realistic values for these load values.

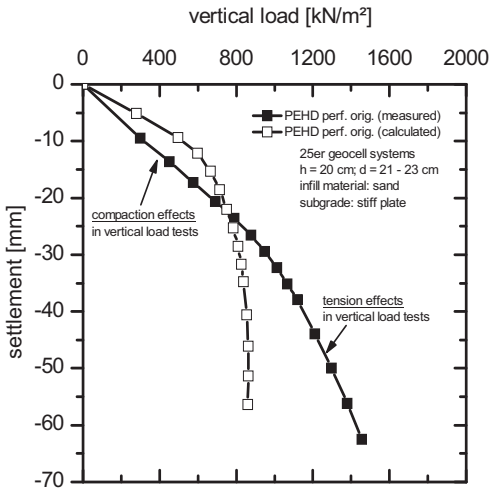

Fig. 9 Comparison of calculated settlements according to Eqs. 9 and 13 and measured settlements for perforated PEHD geocells.

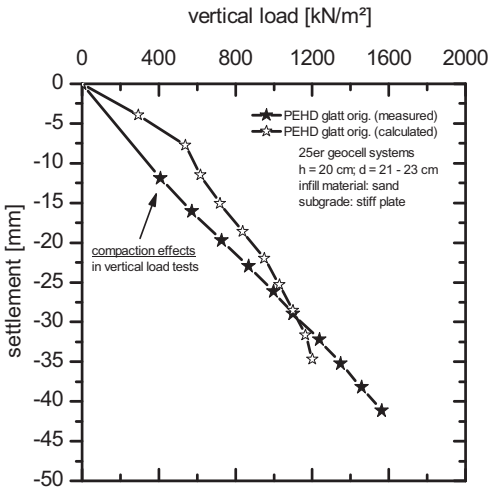

Fig. 10 Comparison of calculated settlements according to Eqs. 9 and 13 and measured settlements for smooth PEHD geocells.

SUMMARY

A new test method called radial load tests has been developed to analyze the load transfer mechanism with a geocell system filled with infill material in detail.

Based on the test results an analytical model has been developed to describe the interconnection between applied load, horizontal earth pressure and hoop stresses within the cell system. The analytical model was verified by comparison of calculated and measured test results. The analytical model was then transferred to a vertical load situation on basis of vertical load test results. Comparison of calculated settlements within a loaded geocell with measured settlements in vertical load tests were in really good agreement. With the described analytical design model settlements within a geocell system can be estimated independent of the geocell or the infill material.

REFERENCES

Bathurst, R.J., Karpurapu, R. (1993). Large scale triaxial compression testing of geocells reinforced granular soils. Geotechnical Testing Journal, ASTM, 16: 296 – 303.

Emersleben A., Meyer N. (2008). The use of geocells in road constructions - Falling weight deflector and vertical stress measurements EuroGeo 4, Proc. 4th European. Geosynthetics Conference EuroGEO4, Edinburh, Scotland.

Emersleben A. (2010). Load Transfer Mechanism of Geocells for the Stabilization of Mineral Base Courses at Static and Cyclic loading. PhD-Thesis at Clausthal University of Technology, ISBN 3-938924-13-6.

Hughes, J.J. (1999). Final Report: Geocell Subgrade Stabilization. Pennsylvania Department of Transportation (PennDOT), Engineering Technology and Information Division.

Mhaiskar, S.Y., Mandal, J.N. (1993). Soft clay subgrade stabilization using geocells: experimental and finite element investigations. Proc. Intl. Conf. on soft soil engineering, Guangzhou,: 785 - 791

Sitharam, T.G., Siressh, S., Dash, S.K. (2008). Bearing capacity of circular Footings on Geocell sand mattress overlying clay bed with voids. Geotextiles and Geomembranes, 27 (2): 89 - 98.

Wesseloo, J., Visser, A.T., Rust, E. (2009). The stress-strain Behavior of multiple geocell packs. Geotextiles and Geomembranes, 27: 31 – 38.